International Journal of Fatigue 113 (2018) 401–406

Contents lists available at ScienceDirect

International Journal of Fatigue

journal homepage: www.elsevier.com/locate/ijfatigue

Technical note

A grain boundary interaction model for microstructurally short fatigue cracks

S. Panwar[a,b], J.F. Adams[a,c], J.E. Allison[a,c], J.W. Jones[a,c], V. Sundararaghavan[a,b,*]

[a] PRedictive Integrated Structural Materials Science (PRISMS) Center, USA
[b] Department of Aerospace Engineering, University of Michigan, Ann Arbor, USA
[c] Department of Material Science, University of Michigan, Ann Arbor, USA

ARTICLE INFO

Keywords:
Grain boundaries
Fatigue
Microstructurally short cracks
Magnesium alloys

ABSTRACT

In this paper, we present a phenomenological model for simulating the effect of a grain boundary on crack growth along crystallographic planes. This model combines various geometrical features of the interaction between the crack plane and the grain boundary plane. The tilt and twist misorientations, calculated at a grain boundary, between a crack plane and a favorable plane in the next grain are incorporated into this model, as are the Schmid factor of the next grain and a critical crack transmission stress. A model calibration procedure is demonstrated based on experimental short fatigue crack growth data measured in a high performance wrought magnesium alloy. The proposed combined GB interaction model is shown to accurately predict the short fatigue crack growth retardation and arrest at grain boundaries in this alloy.

1. Introduction

Microstructural features, such as precipitates, phase boundaries, and grain boundaries (GBs), play an important role in determining the fatigue crack growth behavior of metals and alloys ([1,2]). This is especially true for short fatigue cracks growing along crystallographic planes ([3–5]). GBs can cause the short fatigue crack to retard and, in some cases, arrest. Thus, understanding the interaction between GBs and propagating short cracks is important for accurate prediction of fatigue life.

Many models have been proposed to understand this interaction, most of which have some basis in Bilby, Cottrell, and Swinden's (BCS) theory [6]. However, these models consider the GB as a constraint on the movement of dislocations that are generated at the crack tip, while the geometrical features (e.g. twist and tilt misorientations) of the GB are not taken into consideration. The constraint is modeled either by applying a boundary stress ([7,8]) or a microscopic stress intensity factor [9]. More recently, various phenomenological GB models ([10–12, 18]) have been proposed to combine the geometrical features of the GB with a boundary stress or a microscopic stress intensity factor. These models only consider one geometrical feature of this interaction and neglect the contributions from other geometrical features and the couplings between these features.

In the present study, we propose a combined grain boundary interaction model that takes into account the coupling between the tilt and twist misorientations (which are located between the crack plane and a favorable plane in the next grain, calculated at a grain boundary), the Schmid factor, and the critical crack transmission stress, which is a form of a microscopic stress intensity factor. In Fig. 1, the loading axis is along the global X direction and the crack grows from slip plane 1 to slip plane 2 across a grain boundary. As shown in the figure, two parameters define the misorientations between the slip plane 1 and slip plane 2. The first parameter is called the tilt misorientation, which is the acute angle between the traces of the slip planes on the sample surface. The second parameter is the twist misorientation, which is the angle between the traces of the slip planes on the GB plane. Thus, the twist misorientation is also dependent on the GB orientation (its tilt and rotation). This GB interaction model is combined with the Navarro-De Los Rios (N-R) [7] model to predict the crack growth retardation or arrest when the plastic zone is impinging on a grain boundary, while the BCS model [6] is used to predict crack growth when the plastic zone in front of the crack tip is completely inside a grain. An experimental technique [14] that introduces short fatigue cracks oriented on basal planes in grains with GB misorientations of interest is used to compare the short crack growth rate predictions from the proposed GB interaction model to the measured crack growth rates.

2. Experimental procedure

A wrought rare-earth-containing magnesium alloy, WE43, with a

* Corresponding author at: Department of Aerospace Engineering, University of Michigan, Ann Arbor, USA.
E-mail address: veeras@umich.edu (V. Sundararaghavan).

https://doi.org/10.1016/j.ijfatigue.2018.04.029
Received 15 January 2018; Received in revised form 23 April 2018; Accepted 26 April 2018
Available online 28 April 2018

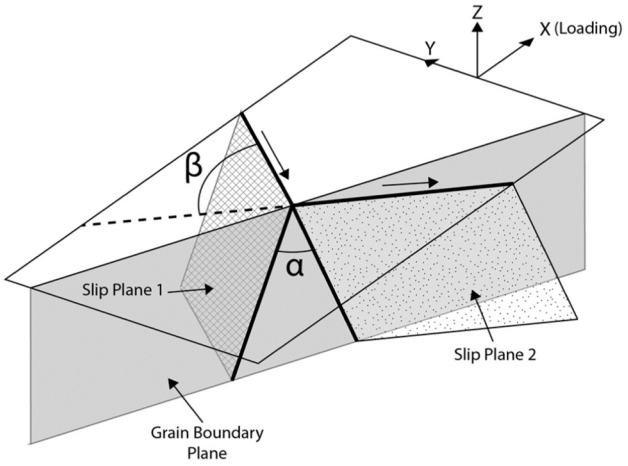

Fig. 1. Crystallographic mechanism for crack growth from Slip Plane 1 to Slip Plane 2.

composition (wt.%) of 3.74Y, 2.10Nd, 0.52Gd, 0.45Zr, 0.016Zn, and Mg (balance) was used for the fatigue crack growth experiments. The as-received material was solution treated at 525 °C for 8 h to produce an average grain size of 113 μm and aged at 250 °C for either 4 or 16 h.

Crystallographic orientation and texture were measured using electron backscatter diffraction (EBSD) in a Tescan Mira3 scanning electron microscope (SEM), which revealed a medium strength basal texture, with an average of 3.7 multiples of random distribution. Basal poles were aligned parallel to the normal direction of the plate, or perpendicular to the loading direction.

Short crack growth behavior was investigated using ultrasonic fatigue, the details of which are described in [14] and [19]. Cylindrical and thin foil specimens of coarse-grained WE43 magnesium alloy were examined in order to understand the effect of grain boundaries on short fatigue crack growth. Electropolished cylindrical specimens featured diametrically opposed gage flats for the characterization of microstructure and observation of fatigue crack growth behavior. Micro-notches were machined in the gage flats to act as crack initiation sites near GBs of interest using a FEI Quanta 200 3D equipped with a gallium ion source focused ion beam (FIB). The micro-notches were 100 μm wide and 40 μm deep. To produce fatigue crack growth along known crystallographic planes, and to allow for the calculation of tilt and twist misorientations, all notches were machined parallel to basal planes in selected grains. Locations for micro-notches were selected based on a variety of microstructural factors characterized using EBSD maps of the specimen gage flats. Initiation sites were chosen in grains with desired combinations of neighbor grain misorientation, size, and basal Schmid factor, to facilitate initial crack growth. Crack growth tests were conducted at a frequency of 20 kHz and at a stress ratio of $R = -1$ at room temperature in laboratory air, with a constant maximum stress of 85 MPa. Observations of fatigue crack growth were made using either an optical system or a Tescan Mira3 SEM. Dog-bone-shaped thin foil specimens with a nominal thickness of 300 μm were fabricated from underaged WE43 in order to reduce the effect of subsurface microstructure on the interaction between the short fatigue crack growth and the GB. The foil specimens were flat coupons 30.5 mm in total length with a 1.6 mm long and 2 mm wide gage section. The longitudinal direction of the specimens was aligned with the rolling direction of the WE43 plate. Specimens were hand-polished to a thickness of approximately 200 μm using SiC paper, and then further thinned to approximately 150 μm through electropolishing, using the same electrolyte used to prepare cylindrical samples. An edge notch perpendicular to the tensile axis was produced at the longitudinal center of the gage section of each fatigue specimen by FIB machining using an FEI Nova 200 nanolab SEM/FIB operating at 30 kV and a probe current of 5.0 nA. Greater detail regarding the experimental techniques can be found in Adams et al. ([14,19]). In the foil specimens, the effect of GBs on the crack growth rate was investigated through characterization of both the surface and subsurface microstructures. For some GBs in the cylindrical specimens, a combination of quantitative fractography and free-surface observation enabled the identification of GB orientation in three dimensions (Fig. 2). However, in Fig. 3a, only surface observation techniques were used to calculate the twist misorientations. This calculation uses the rudimentary assumption that the GB plane lies perpendicular to the specimen free surface. The accuracy of this assumption is dependent on microstructural features that vary with material, but it is necessary when using a two-dimensional characterization of a three-dimensional process. In Fig. 4a, using three-dimensional GB orientation, twist misorientations were calculated, and they were found to be minimally different than those calculated using the perpendicular boundary assumption.

Early surface crack propagation was found to consist primarily of crystallographic transgranular growth predominantly along basal planes, with non-crystallographic transgranular growth occurring occasionally at longer crack lengths. Fatigue crack growth behavior near GBs was characterized by frequent retardation (Fig. 4a) of crack growth rates and occasional crack arrest (Fig. 3a). Details on two specific cases of fatigue crack growth in cylindrical and thin foil specimens, along

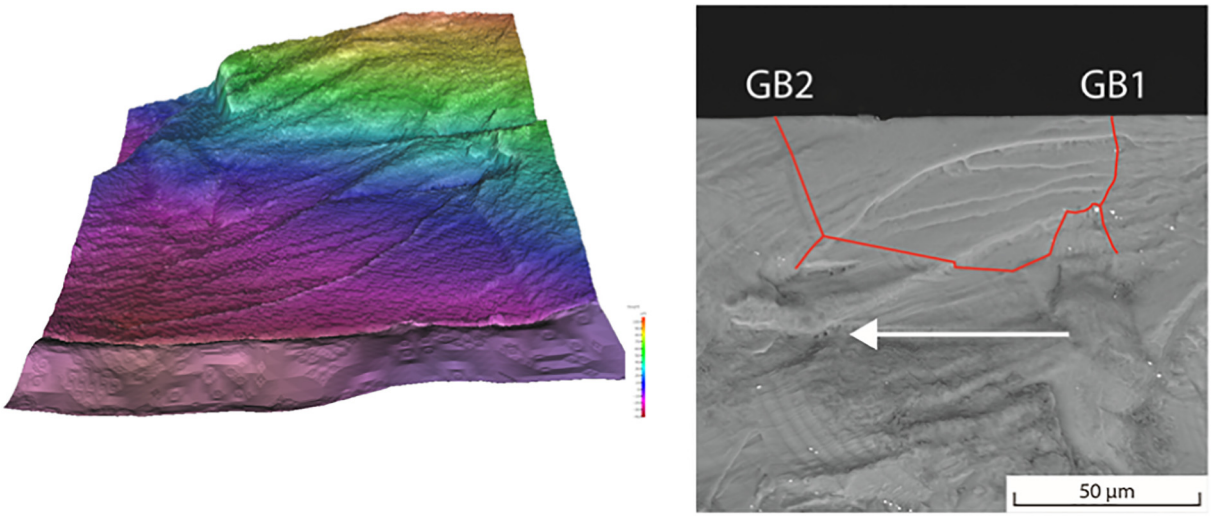

Fig. 2. Twist misorientation from 3D quantitative fractography in a cylindrical specimen.

with a discussion of the efficacy of the proposed model in describing the observed behavior, are discussed further in the results and discussion section.

3. Review of existing grain boundary interaction models

Zhai et al. [10] (Fig. 1) conducted micro-scale experiments to show the effects of the tilt (β) and twist (α) misorientations between the crack plane (Slip Plane 1) and the adjacent grain slip plane (Slip Plane 2) on short fatigue crack growth. They found that the microstructurally short crack growth rate appeared to be influenced by tilt misorientation, twist misorientation, Schmid factors, and other GBs that are interacting with the crack. Wen and Zhai [12] introduced a model that assumes that the resistance offered by the GB due to the twist misorientation is in the form of a Weibull-type function.

Luster and Morris [18] investigated slip transfer across GBs using a geometric compatibility factor m′, defined as

$$m' = \cos\kappa\cos\phi \tag{1}$$

where κ is defined as the angle between the slip vectors of two adjacent grains and ϕ is the angle between the slip plane normal to those grains. A low value of m′ indicates an increased difficulty of slip transfer. The geometric compatibility factor allows for quick investigation of the resistance of the GB; however, it fails to take into account the effect of the GB orientation on the GB barrier strength.

Wilkinson's model [11] incorporates the effects of the adjacent grain orientation and the twist misorientation. The adjacent grain orientation effect is considered using the ratio of the Sachs factor of Slip Plane 1 ($m_{current}$) to the Sachs factor of Slip Plane 2 (m_{next}). The critical stress, $S(r_0)$, is the stress required for a crack to cross a GB. To prevent stress singularities, it is determined at a distance r_0 from the GB in the adjacent grain. It is given by

$$S(r_0) = \frac{m_{next}}{m_{current}}\left[1 + \frac{\alpha}{\alpha_0}\right]\frac{S_{ct}(r_0)}{2} \tag{2}$$

S_{ct} is the critical stress required for crack transmission (ct) across a grain boundary without a change in the direction of the crack path, and α_0 is a calibration parameter.

4. Proposed combined GB interaction model

Our proposed combined GB interaction model consists of some features of existing GB interaction models with modifications that help us to accurately predict short crack growth retardation and arrest at a GB. Experiments [10] reveal that both the tilt and twist misorientations play a role in slip transmission; thus, we incorporate features of both the Wilkinson Model (Eq. (2)) and the Wen and Zhai Model [12].

We assume that the ratio of the Schmid factor of the current grain and that of the next grain, the tilt and twist misorientations, and the critical crack transmission stress directly affect the short crack growth rates. Thus, the critical stress S (the stress required for a crack to cross a GB) at a distance r_0 from the GB is given by,

$$S(r_0) \geqslant f(M) f(\alpha,\beta) f(S_{ct}) \tag{3}$$

$$f(M) = \frac{M_{current}}{M_{next}}$$

Here, M is the Schmid factor. The form of the tilt and twist misorientation function is more involved since the twist misorientation has a larger effect on crack growth than the tilt misorientation. This effect can be simulated with an exponential distribution as shown:

$$f(\alpha,\beta) = \left[\frac{1-e^{-\left(\frac{1-\cos\beta}{\alpha_1}+\frac{\sin\alpha}{\sin\alpha_2}\right)}}{1-e^{-\left(\frac{1}{\alpha_1}\right)}}\right] \tag{4}$$

The numerator of this function is similar to Wen and Zhai Model [12], except that the tilt and twist misorientations are now coupled and a weighting parameter α_1 is applied to scale the effect of twist misorientation in relation to tilt misorientation. The normalization of this function is based on half the maximum value of the tilt misorientation (90°) and the minimum value of the twist misorientation (0°). This is the case for a crack path that is changing from intergranular to transgranular.

Krupp et al. [13] have shown a way to calculate the value of $f(S_{ct})$:

$$f(S_{ct}) = \frac{k_l}{M_{current}\sqrt{r_0}} \tag{5}$$

Here, k_l is a locking parameter from the Hall-Petch relationship for tensile yield strength. The term r_0 is included to prevent a stress singularity, and value between 0.1 and 1 μm is typically used [15].

Thus, Eq. (3) becomes:

$$S(r_0) \geqslant \frac{k_l}{M_{next}\sqrt{r_0}}\left[\frac{1-e^{-\left(\frac{1-\cos\beta}{\alpha_1}+\frac{\sin\alpha}{\sin\alpha_2}\right)}}{1-e^{-\left(\frac{1}{\alpha_1}\right)}}\right] \tag{6}$$

Eq. (6) is combined with the BCS [6] and the N-R [7] models to predict short crack growth. In these models, the crack growth rate is assumed to be proportional to the crack tip sliding displacement ($\Phi(a)$).

$$\frac{da}{dN} = \lambda\Phi(a)^m \tag{7}$$

This assumption has been used in numerous analytical short fatigue crack growth models ([8,9,11,13]). In our combined GB interaction model, for simplicity, $m = 1$ and λ is calibrated for each material condition. The value of the parameter λ lies between zero and one, which correspond to completely reversible slip and completely irreversible slip, respectively. No attempt has been made to model the crack growth itself; rather, the effectiveness of the proposed combined GB interaction model in capturing crack growth retardation and crack arrest at a GB is presented.

5. Results and discussion

In this section, the three crack-GB interaction models, described in the previous sections, are compared using the experimental fatigue crack growth rates determined from testing of cylindrical and thin foil specimens. In both types of specimens, the crack growth was predominantly crystallographic in nature. The most significant difference between the thin foil specimens and the cylindrical specimens was a significant reduction in noncrystallographic transgranular crack growth in the thin foil specimens. In the next few paragraphs, the fatigue crack growth rates of two cylindrical specimens are shown along with the combined GB model and Wilkinson's model. Only the experimental crack growth along the basal slip system is selected for the comparison due to large variations in the values of the critical resolved shear stresses for different slip systems in magnesium. In order to make a fair comparison between the three crack-GB interaction models, we use a retardation factor in the last part of this section to show the effect of GBs on the crack growth rate. The retardation factor is evaluated by dividing the lowest crack growth rate observed as the crack approaches the GB (da/dN_{GB}) by the approximate steady state crack growth rate in the grain (da/dN_{ss}). The value of this retardation factor ranges from 0 to 1, with 0 indicating permanent crack arrest and 1 indicating no observed effect of the GB on the crack growth rate.

The material properties and model parameters of WE43 alloy are shown in Table 1.

In Fig. 3a, the notch was placed in a grain with a basal Schmid factor of 0.5. The left end of the notch was located 64 μm, measured along the surface basal trace, from GB 1. The right end of the notch was located 59 μm, measured along the surface basal trace, from GB 2. In Fig. 3b, crack growth arrests at GB 1 due to the large twist misorientation, while, in Fig. 3c, both the tilt and twist misorientations

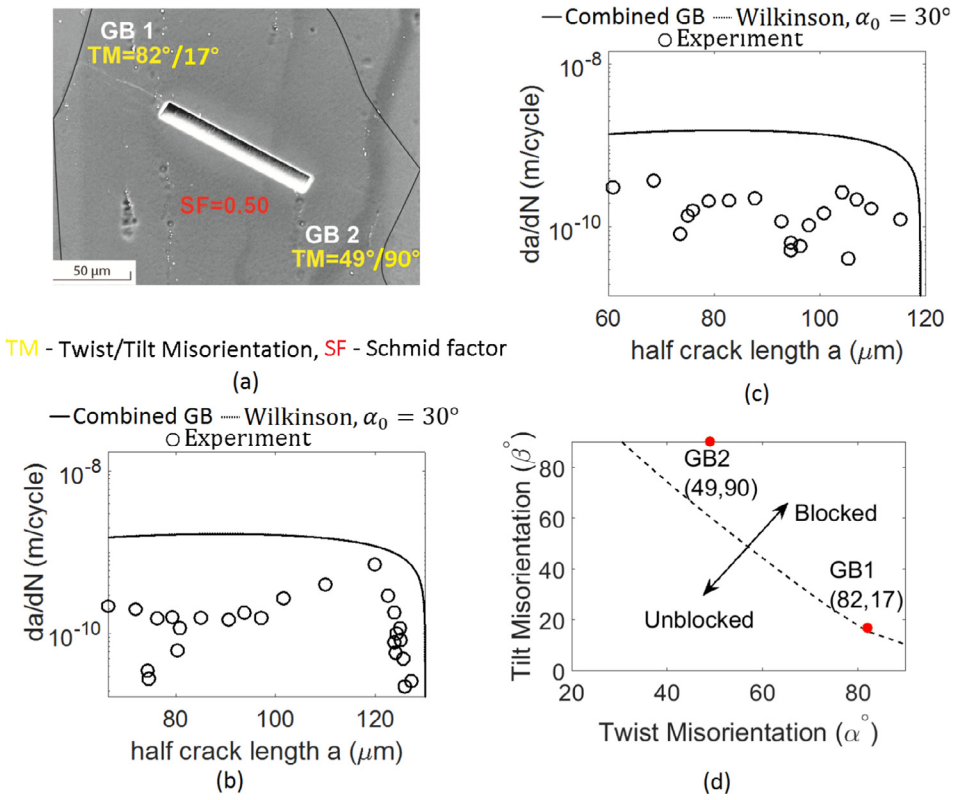

Fig. 3. GB interaction models (Eqs. (2) and (6)) and experimental [14] fatigue crack growth data for an arresting crack on both sides of the notch. (a) SEM image of notch and fatigue crack with tilt (β), twist (α) misorientations, and Schmid factor (SF) values. The grain boundaries are assumed perpendicular to the surface. (b) Calibration curves representing the crack growth to the left of the notch (GB1). (c) Prediction curves of different GB interaction models representing the crack growth arrest to the right of the notch (GB2). (d) Plot of Tilt vs Twist misorientations corresponding to $\alpha_1 = 1.41$, showing various values of tilt and twist misorientations for which the crack growth is blocked at the GB.

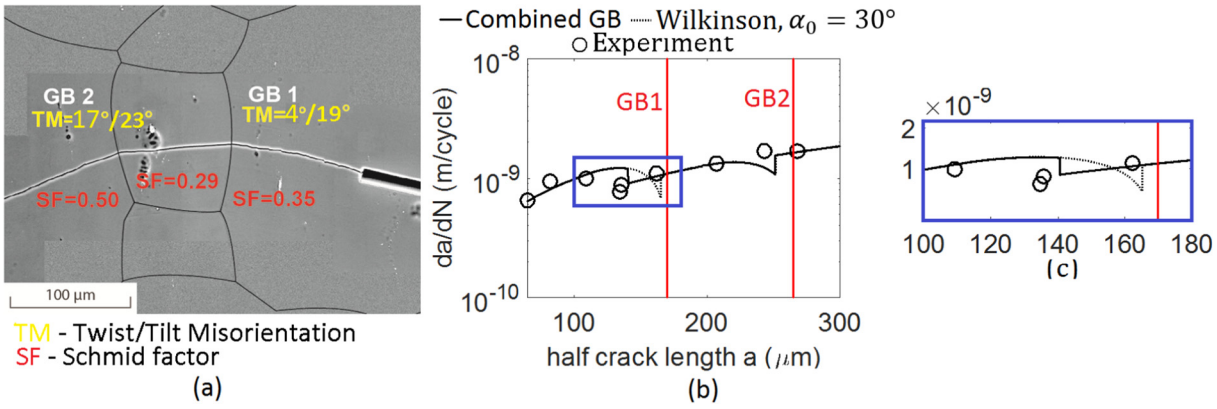

Fig. 4. Crack growth retardation predictions. (a) SEM image showing crack passing through two GBs with tilt (β), twist (α) misorientations, and Schmid factor (SF) values. The grain boundary angles are calculated by 3D quantitative fractography (Fig. 2). (b) Crack growth rate predictions with crack deaccelerating at GB 1 and GB 2. (c) Zoomed-in view of crack deacceleration near GB 1.

cause the crack growth to arrest. In Fig. 3b, the combined GB interaction model is calibrated by varying α_1 to get the desired fit, resulting in a value of 1.41. This is the minimum value of α_1 that produces crack arrest. The same figure is used to calibrate Wilkinson's model by varying α_0 to get the best fit value of 30°. In Fig. 3c, using these calibrated parameters, the combined GB interaction model (Eq. (6)) and Wilkinson's model (Eq. (2)) predict the crack growth arrest event. In Fig. 3d, a plot of tilt vs twist misorientations is shown for $\alpha_1 = 1.41$. This plot shows the different combinations of the tilt and twist misorientations that will block the crack growth.

Table 1
Magnesium alloy WE43 properties and interaction model parameters.

μ(GPa)	ν	b(Å)	α_2(°) (*basalslip*) [12]	λ ($cycle^{-1}$)	r_0(μm) (*assumed*)	k_I(MPa$\sqrt{mm}$) [16]	τ_f(MPa) (*basal*) [17]
17.32	0.27	3.21	45	0.004	0.1	6.96	55

Table 2
Comparison between the different crack-GB interaction models using cylindrical specimens.

Specimen	GB	Tilt (°)	Twist (°)	SF1	SF2	D1 (μm)	D2 (μm)	m′	RF (Combined GB)	RF (Wilkinson)	RF (Exp)
1	1	17	82	0.50	0.48	260	120	0.12	0.00	0.00	0.00
1	2	90	49	0.50	0.42	260	80	0.04	0.00	0.00	0.00
2	1	19	4	0.35	0.29	340	95	0.88	0.82	0.80	0.78
2	2	23	17	0.35	0.50	95	200	0.85	0.90	0.81	1.00

Table 3
Comparison between the different crack-GB interaction models using thin foil specimens.

Specimen	GB	Tilt (°)	Twist (°)	SF1	SF2	D1 (μm)	D2 (μm)	m′	RF (Combined GB)	RF (Wilkinson)	RF (Exp)
1	1	86	36	0.5	0.49	191	108	0	0.55	0.46	0.67
1	2	54	51	0.49	0.15	108	359	0.53	0.00	0.00	0.15
2	1	78	46	0.5	0.28	181	100	0.02	0.10	0.00	0.47

In Fig. 4a, the notch was placed in a grain with a basal Schmid factor of 0.35. The left edge of the notch was located 111 μm, measured along the surface basal trace, from GB 1. GB 2 was located 95 μm from GB 1. The right edge of the notch was located near a series of finer grains not characterized for misorientation. At GB 1, the crack growth rate slows due to the 19° tilt misorientation, as shown in Fig. 4b. The current GB interaction model includes this tilt misorientation and it closely captures the location of this deacceleration, as shown in Fig. 4c. Wilkinson's model over-predicts this location.

In Table 2, the retardation factors for the cylindrical experiments [19], RF (Exp), are compared with the retardation factors for the combined GB model, RF (Combined GB), and for Wilkinson's model, RF (Wilkinson).

In Table 3, the retardation factors from the thin foil experiments are compared with those determined from the combined GB model and Wilkinson's model. Looking at Table 2, the RF values from the three crack-GB models (the combined GB model, Wilkinson's model, and the m′ model) predict the general crack growth retardation trend observed in the experiments. This general crack growth retardation trend is also consistent with the trend of the twist misorientation, with higher twist corresponding to a lower crack growth rate. However, when we look at the thin foil data in Table 3, the difference in the crack growth retardation predictions from the three models become clear. If we consider the tilt and twist misorientations separately, their individual effect on crack growth retardation is not clear; however, as compared to the tilt misorientation, the twist misorientation does has a greater effect on the crack growth retardation. Thus, we might consider the prospect of some unequal coupling between the tilt and twist misorientations. This unequal coupling is representation by our combined GB model. As shown in both tables, there does not appear to be a clear link between the m′ parameter and the crack growth retardation.

In Fig. 5, all of the data presented in this paper are plotted with respect to tilt and twist misorientations. Solid points in the figure indicate that the crack growth was blocked at the GB and empty points indicate that the crack growth was either retarded or unaffected by the presence of the GB. The points highlighted in red show the mismatch between the models' prediction and the experiments. The Schmid factors of the second grain for each of the data shown in the tables are also plotted. Few points to be made here are: (1) all models work at low twist and tilt misorientations, where crack is transmitted, (2) m′ parameter fails at high twist misorientation where we expect the crack to get blocked, (3) Wilkinson's model fails at one of the high tilt misorientation cases, and (4) both Wilkinson's model and the present model failed at a midway point of moderate tilt misorientation and moderate twist misorientation where we think the models requires more refinement. A recent investigation [20] on short crack growth in BCC Titanium using statistical techniques has shown that minimization of the residual Burgers vector provided the best predictivity in modeling slip

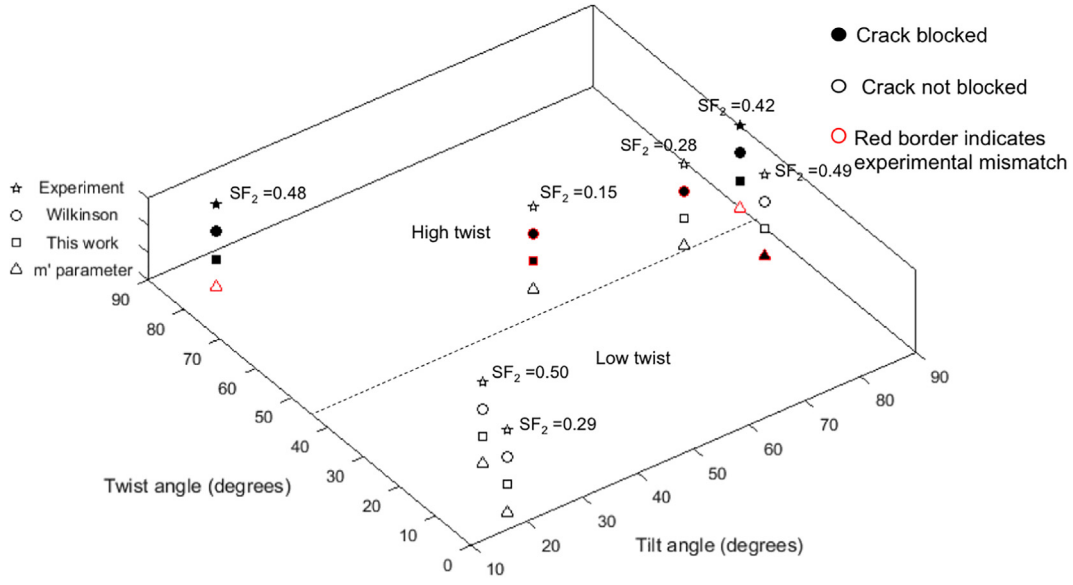

Fig. 5. Comparison between the different crack-GB interaction models using cylindrical and thin foil specimens.

transmission. Given enough statistical data points, we anticipate the use of statistical analysis [20] and learning [21] to investigate factors influencing crack-GB interactions in HCP Magnesium alloys.

The assumption employed in most of the crack-GB interaction phenomenological models is that all the grains experience the same state of stress. Hence, we restricted our analysis to the use of the basal Schmid factor to describe the local stress state. Ideally, multi-slip models (eg. Taylor factor) would have to be employed so that the complex loading state in the grain can be captured. However, such calculation is not straightforward in HCP Mg (as compared to FCC crystals) due to inadequate number of slip systems for accommodating deformation and unequal slip system strengths. Also, we have not taken into account the contributions from the neighboring grains. These neighboring grains may have a strong influence on the local stress state in the cracked grain. In addition, due to the single slip description of our model, we have only compared the basal crack growth retardation and arrest in each of the three models. These are some limitations of our model. However, our results indicate complex coupling between various crack-GB interaction parameters in the prediction of crack growth retardation and arrest at grain scale.

6. Conclusion

In summary, we present a phenomenological model for simulating short fatigue crack growth retardation and arrest at grain boundaries. Unique features of this model include the incorporation of the combined effect of the tilt and twist misorientations into a single exponential function, the use of a Schmid factor to account for loading in the neighboring grain, and the effect of the crack transmission stress. Parameters are calibrated through micro-scale fatigue crack growth experiments from notched samples. Crack growth experiments in WE43 magnesium exhibit a strong interaction between fatigue cracks and grain boundaries. At grain boundaries with lower values of tilt and twist misorientations, fatigue crack growth rates measured on the surface undergo slight retardation or remain unaffected, while, at grain boundaries with higher twist misorientations, fatigue cracks were arrested. These retardations and arrests can be accounted for using this combined GB interaction model and provide a reasonable basis for extension to 3D crack - grain boundary interactions.

Acknowledgments

This research has been conducted as part of the PRedictive Integrated Structural Materials Science (PRISMS) Center at the University of Michigan, funded by the U.S. Department of Energy, Office of Basic Energy Sciences, Division of Materials Sciences and Engineering, under Award no. DE-SC0008637.

References

[1] Lankford J. The growth of small fatigue cracks in 7075–t6 aluminum. Fatigue Fract Eng Mater Struct 1982;5(3):233–48.
[2] Morris W. The noncontinuum crack tip deformation behavior of surface microcracks. Metall Trans A 1980;11(7):1117–23.
[3] Schaef W, Marx M. A numerical description of short fatigue cracks interacting with grain boundaries. Acta Mater 60(5), 2425–36.
[4] Panwar S, Sundararaghavan V. Dislocation theory-based cohesive model for microstructurally short fatigue crack growth. Mater Sci Eng: A 2017;708:395–404.
[5] Schaef W, Marx M. A numerical description of short fatigue cracks interacting with grain boundary. Acta Mater 2012;60(5):2425–36.
[6] Bilby B, Cottrell A, Swinden K. The spread of plastic yield from a notch. In: Proceedings of the royal society of london a: mathematical, physical and engineering sciences, vol. 272, The Royal Society; 1963, pp. 304–14.
[7] Navarro A, De Los Rios E. An alternative model of the blocking of dislocations at grain boundaries. Philosop Mag A 57(1) (1988) 37–42.
[8] De Los Rios E, Xin X, Navarro A. Modelling microstructurally sensitive fatigue short crack growth. In: Proceedings of the royal society of london a: mathematical, physical and engineering sciences, vol. 447, The Royal Society; 1994, pp. 111–34.
[9] Tanaka K, Akiniwa Y, Nakai Y, Wei R. Modelling of small fatigue crack growth interacting with grain boundary. Eng Fract Mech 1986;24(6):803–19.
[10] Zhai T, Wilkinson A, Martin J. A crystallographic mechanism for fatigue crack propagation through grain boundaries. Acta Mater 2000;48(20):4917–27.
[11] Wilkinson AJ, Modelling the effects of microstructure and microtexture on the statistics of short fatigue crack growth. In: ICF10, Honolulu (USA) 2001; 2013.
[12] Wen W, Zhai T. Quantification of resistance of grain boundaries to short-fatigue crack growth in three dimensions in high strength al alloys. Metall Mater Trans A 2012;43(8):2743–52.
[13] Dueber O, Kuekler B, Krupp U, Christ H-J, Fritzen C-P. Experimental characterization and two-dimensional simulation of short-crack propagation in an austenitic–ferritic duplex steel. Int J Fatigue 2006;28(9):983–92.
[14] Adams J, Allison J, Jones W. The effects of heat treatment on very high cycle fatigue behavior in hot-rolled WE43 magnesium IJF, (2016).
[15] Krupp Ulrich. Fatigue crack propagation in metals and alloys: microstructural aspects and modelling concepts. John Wiley & Sons, (2007), Page 221.
[16] Caceres CH, Mann Gemma E, Griffiths JR. Grain size hardening in Mg and Mg-Zn solid solutions. Metall Mater Trans A 2011;42(7):1950–9.
[17] Ganesan S. Microstructural response of magnesium alloys: 3D crystal plasticity and experimental validation, Dissertation. University of Michigan, Ann Arbor, 2017.
[18] Luster J, Morris MA. Compatibility of deformation in two-phase Ti-Al alloys: dependence on microstructure and orientation relationships. Metall Mater Trans A 1995;26(7):1745–56.
[19] Adams J. Investigating microstructural effects on short crack growth and fatigue life behavior of WE43 Magnesium, Dissertation. University of Michigan, Ann Arbor, 2018.
[20] Rovinelli Andrea, et al. Predicting the 3D fatigue crack growth rate of small cracks using multimodal data via Bayesian networks: In-situ experiments and crystal plasticity simulations. J Mech Phys Solids 115 (2018): 208–29.
[21] Sundararaghavan V, Zabaras N. A statistical learning approach for the design of polycrystalline materials. Statist Anal Data Mining: ASA Data Sci J 2009;1(5):306–21.